

Theory of Scanning Tunneling Spectroscopy of Magnetic Adatoms in Graphene

Bruno Uchoa¹, Ling Yang², S.-W. Tsai², N. M. R. Peres³, and A. H. Castro Neto⁴¹Department of Physics, University of Illinois at Urbana-Champaign, 1110 W. Green St, Urbana, IL, 61801, USA²Department of Physics and Astronomy, University of California, Riverside, CA, 92521, USA³Centro de Física e Departamento de Física, Universidade do Minho, P-4710-057, Braga, Portugal and⁴Department of Physics, Boston University, 590 Commonwealth Avenue, Boston, MA 02215, USA

(Dated: February 21, 2024)

We examine theoretically the signatures of magnetic adatoms in graphene probed by scanning tunneling spectroscopy (STS). When the adatom hybridizes equally with the two graphene sublattices, the broadening of the local adatom level is anomalous and can scale with the cube of the energy. In contrast to ordinary metal surfaces, the adatom local moment can be suppressed by the proximity of the probing scanning tip. We propose that the dependence of the tunneling conductance on the distance between the tip and the adatom can provide a clear signature for the presence of local magnetic moments. We also show that tunneling conductance can distinguish whether the adatom is located on top of a carbon atom or in the center of a honeycomb hexagon.

PACS numbers: 73.20.Hb, 71.55.Ht, 73.20.-r

Graphene is a two dimensional sheet of carbons whose remarkable electronic properties derive from the presence of electronic excitations that behave as chiral Dirac quasiparticles [1]. Although clean bulk graphene may not be magnetic, there is a rich variety of possibilities for magnetism when adatoms are added on top of graphene. As an open surface, the use of scanning tunneling microscopy (STM) probes [2] opens the possibility of controlling the position of adatoms with atomic precision [3] and at the same time switching the magnetic local moments on and off by gating [4, 5].

One of the challenges for the manipulation of local moments is about detection: how can one reliably identify a local magnetic moment at room temperature. Unlike ordinary metal surfaces, due to the low density of states (DOS), an adatom localized level can hybridize strongly with the STM tip. We propose that the dependence of the adatom STM differential conductance (DC) with the distance to a non-magnetic STM tip, in the limit of small separation, can provide an experimental signature for the presence of local moments above the Kondo temperature [6]. Furthermore, because the electrons in graphene carry different sublattice quantum numbers, we show that when the adatom sits in the center of the honeycomb hexagon [see Fig. 1 (b)], destructive interference between the different tunneling paths changes substantially the form of the Fano factor [7] and the shape of the DC curves compared to the case where the adatom is located on the top of a carbon atom [Fig. 1 (a)]. This effect allows the use of STM to characterize adatoms and defects in graphene, including substitutional impurities in single and double vacancies [8].

Our starting point is the free Hamiltonian of the graphene/adatom/tip system: $H = H_g + H_f + H_c$. H_g is the tight-binding Hamiltonian for graphene: $H_g = \sum_{ij} t_{ij} a_i^\dagger b_j + \text{h.c.}$; where a, b are the fermionic operators for sublattices A and B, respectively

($t = 2.8 \text{ eV}$), and $s = \pm 1/2$ is the spin. In momentum space,

$$H_g = \sum_{\mathbf{k}} t_{\mathbf{k}} (a_{\mathbf{k}}^\dagger b_{\mathbf{k}} + b_{\mathbf{k}}^\dagger a_{\mathbf{k}}); \quad (1)$$

where $t_{\mathbf{k}} = \frac{1}{3} \sum_{i=1}^3 e^{i\mathbf{k} \cdot \mathbf{a}_i}$, $a_1 = \hat{x}$, $a_2 = \frac{\sqrt{3}}{2} \hat{x} + \frac{1}{2} \hat{y}$, and $a_3 = \frac{\sqrt{3}}{2} \hat{x} - \frac{1}{2} \hat{y}$ are the lattice nearest neighbor vectors. $H_c = \sum_{\mathbf{k}} c_{\mathbf{k}}^\dagger c_{\mathbf{k}}$; $c_{\mathbf{k}}$ is the effective Hamiltonian for the tip electrons, with $\epsilon_{\mathbf{k}} = (\mathbf{k}^2)/2m_D$, where m is the effective electronic mass, and ϵ_D is the energy at the bottom of the tip band with respect to the Dirac point, and $H_f = \epsilon_f f^\dagger f$ is the Hamiltonian of the f electrons at the local level with energy ϵ_f . The Coulomb energy, U , for double occupancy of the local level is described by a Hubbard term: $H_U = U f_{\uparrow}^\dagger f_{\uparrow} f_{\downarrow}^\dagger f_{\downarrow}$. Since we are only interested in the magnetic state of the adatom (we do not include the Kondo effect and hence our theory is valid above the adatom Kondo temperature, T_K), in what follows we use Anderson's mean field decomposition [4]: $H_{U, MF} = U \langle n \rangle f_{\uparrow}^\dagger f_{\uparrow} U \langle n \rangle$; where $\langle n \rangle = \langle f_{\uparrow}^\dagger f_{\uparrow} + f_{\downarrow}^\dagger f_{\downarrow} \rangle$ is the average occupation of the f level. Hence, at the mean field level we write: $H_{f, MF} = \epsilon_f f^\dagger f$; where $\epsilon_f = \epsilon_f + U \langle n \rangle$ is the renormalized level energy.

In graphene the adatoms can be localized at different

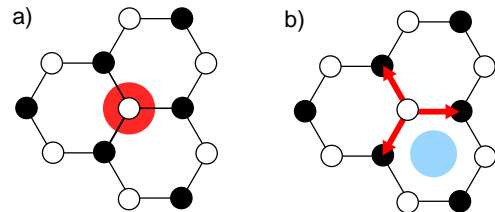


FIG. 1: Two adatom positions in graphene: a) asymmetric case, on top of a carbon atom, when the adatom (large circle) hybridizes with one sublattice and b) symmetric case, when the adatom is located at the center of a hexagon. Red arrows: nearest neighbor vectors.

positions in the honeycomb lattice [8]. Here we consider two cases where the adatom is either placed on top of a carbon atom, in which case the sublattice symmetry is locally broken, or the adatom is located in the center of an hexagon without symmetry breaking. In the first case, assuming the adatom to be on the B sublattice, we have: $H_{V;AS} = V_P \sum_{\mathbf{p}} \frac{f^y b}{3} (0) + h\kappa$. In the second case we have: $H_{V;S} = \sum_{i=1}^3 V a^y(a_i) + b^y(-a_i) f + h\kappa$. In momentum space, these two terms can be written as:

$$H_{V;AS} = V \sum_{\mathbf{p}} b_{\mathbf{p}}^y f + h\kappa \quad (2)$$

in the asymmetric case, and

$$H_{V;S} = V \sum_{\mathbf{p}} (b_{\mathbf{p}}^y + a_{\mathbf{p}}^y) f + h\kappa \quad (3)$$

in the symmetric one [9].

In the presence of an STM tip, there are two additional hopping terms: $H_{fc} = V_c \sum_{\mathbf{r}} f^y c(\mathbf{r}) + h\kappa$, where V_c is the effective tunneling energy between the tip and the adatom, and $H_{gc} = \sum_{i,j} t_{c,ij} a^y(R_i) + b^y(R_i) c(R_j) + h\kappa$; where $t_{c,ij}$ is the hopping energy between the tip and each carbon, $\mathbf{r} = (R; z)$ is the position of the tip with respect to the adatom, R is the in-plane distance from the adatom to the center of the tip, and z is the out-of-plane distance between them. The fact that the adatom sits a few angstroms above the graphene plane is accounted by the exponential z dependence of the tunneling energies. In momentum space we have: $H_{fc} = V_c \sum_{\mathbf{p}} f^y c_{\mathbf{p}} + h\kappa$; and $H_{gc} = \sum_{\mathbf{k}, \mathbf{p}} t_{c,p}(\mathbf{r}) a_{\mathbf{p}}^y + b_{\mathbf{p}}^y c_{\mathbf{k}} + h\kappa$; where $t_{c,p}(\mathbf{r}) = t_c(z) e^{i\mathbf{p} \cdot \mathbf{R}}$ after averaging over the position of the carbon sites below the impurity.

In the absence of the tip, after diagonalization of the Hamiltonian $H_g + H_f + H_v$ in Eq. (1)-(3), the retarded Green's function of the f electrons $G_{ff}^R(\omega) = \text{HT}[\langle f(\omega) f(0) \rangle]$ is given by:

$$G_{ff}^R(\omega) = [\omega - \Sigma_{ff}^R(\omega)]^{-1} \quad (4)$$

where $\Sigma_{ff}^R(\omega)$ is the self-energy of the localized electrons due to the hybridization with the electrons in graphene. As in the usual Anderson impurity problem [10], the formation of local moments is defined by the occupation of the localized level n for up and down spins, $n = \langle f^\dagger f \rangle = \text{Im} G_{ff}^R(\omega) / \pi$; where ω is the chemical potential ($\omega \approx 7$ eV is an energy cut-off).

In the asymmetric case [see Eq.(2)], $\Sigma_{ff}^R(\omega) = V^2 \sum_{\mathbf{p}} G_{bb;p}^R(\omega)$, where $G_{bb}^R(\omega) = \text{HT}[\langle b(\omega) b(0) \rangle]$ is the diagonal component of the bare graphene Green's function, G_{xy} , with $x, y = a, b$:

$$G_{xy;k}^R(\omega) = \frac{t_{xy}^0 + t_{xy}^1 \text{Re}(\omega) + t_{xy}^2 \text{Im}(\omega)}{t_{xy}^2 \omega^2 + t_{xy}^1 \omega + t_{xy}^0}; \quad (5)$$

where t_j ($j = 1, 2$) are off-diagonal Pauli matrices ($t_{ba}^2 = t_{ab}^2 = i$), and t^0 is the identity matrix. We calculate the

self-energy within the linearized theory, where the energy around the K (K^0) point is given by: $\epsilon(\mathbf{k}) = v_F k$, where $v_F \approx 10^6$ m/s is the Fermi velocity. It reads [4]:

$$\Sigma_{ff}^{AS}(\omega) = \omega \ln D^2 - \omega^2 \int_{-D}^D \frac{d\omega'}{\omega'} \quad (6)$$

where $D = (V/D)^2$ is the dimensionless hybridization parameter. The imaginary part of (6) gives the broadening of the level due to the hybridization of the adatom, and it is proportional to the DOS of the host.

In the symmetric case, however, the hybridization of the f electrons is mediated by the virtual hopping of the electrons in graphene into a "ghost" site located below the adatom, in the center of the hexagon. In this process, as the electrons hop in and out from the adatom, they gain an additional phase that leads to interference between the different quantum mechanical paths involving the six adatom neighboring sites on both sublattices. The self-energy in this case involves also off-diagonal terms of (5):

$$\Sigma_{ff}^S(\omega) = V^2 \sum_{\mathbf{p}} [(b_{\mathbf{p}}) a_{\mathbf{p}}(\omega) + (a_{\mathbf{p}}) b_{\mathbf{p}}(\omega)]; \quad (7)$$

where $a_{\mathbf{p}}(\omega) = (b_{\mathbf{p}}) G_{xb;p}^{0R}(\omega) + (a_{\mathbf{p}}) G_{xa;p}^{0R}(\omega)$. In the linearized theory, Eq. (7) gives [11]:

$$\Sigma_{ff}^S(\omega) = \omega \ln D^2 - \omega^2 \int_{-D}^D \frac{d\omega'}{\omega'} \quad (8)$$

where $D^2 = 1 - (1 - \omega) \text{Re} \Sigma_{ff}^S(\omega) = 1 + 2\omega^2 \ln D^2 + \omega^2 \ln D^2 - \omega^2 \int_{-D}^D \frac{d\omega'}{\omega'}$ gives the quasiparticle residue. The imaginary part of Σ_{ff}^S gives rise to an anomalous broadening of the adatom level that scales with $|\omega|^3 = \omega^2$, suppressing strongly the hybridization when $|\omega| \rightarrow 0$.

In the perturbative regime where V_c, t_c are small compared to V , the inclusion of the tip leads to an additional renormalization of the f electrons Green's function, $G_{ff}^R(\omega) = G_{ff}^R(\omega) + G_{ff}^{(1)}(\omega)$, where

$$G_{ff}^{(1)}(\omega) = V_c(\omega) V_c(\omega) \sum_{\mathbf{k}} G_{cc;k}^{0R}(\omega) \quad (9)$$

$G_{cc;k}^{0R}(\omega) = [\omega - \epsilon(\mathbf{k}) + i0^+]^{-1}$ is the retarded Green's function of the c -electrons, $G_{cc;k}^0(\omega) = \text{HT}[\langle c(\omega) c_k^\dagger(0) \rangle]$, whereas $V_c(\omega)$ is the renormalized tunneling energy between the tip and the adatom, namely

$$V_c^{AS}(\omega) = V_c + V t_c(z) G_{ab}^{0R}(\omega) + G_{bb}^{0R}(\omega) \quad (10)$$

for the asymmetric case, where $V_c(\omega)$ follows from the exchange $G_{xb}^0 \rightarrow G_{bx}^0$, and

$$V_c^S(\omega) = V_c + V t_c(z) [a(\omega) + b(\omega)] \quad (11)$$

in the symmetric one ($V^S = V^S$). In our notation, $(R) = \sum_{\mathbf{p}} e^{i\mathbf{p} \cdot \mathbf{R}} x_{\mathbf{p}}$ is the Fourier transform of x .

$G_{ff}^{(1)}$ in Eq. (9) can be easily computed assuming an effective band width, D , for the c electrons in the tip.

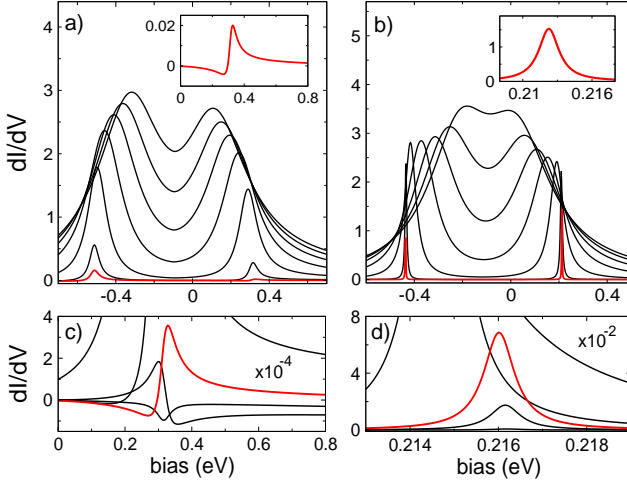


FIG. 2: A adatom induced DC, $G = dI/dV$, versus bias when the adatom sits (left) on top of carbon and (right) in the center of the hexagon. See details in the text. a), b) $t_c = 0.15\text{eV}$ and $V_c/t_c = 1.6, 1.5, 1.35, 1.1, 0.7, 0.25$ and 0.1 (inset), from top to bottom. c), d) $t_c = 0.02\text{eV}$ and $V_c/t_c = 0.7, 0.25, 0.1, 0.05$ and 0.01 . $V_c/t_c = 0.1$ for all curves in red.

The adatom induced DC is $G(r;!) / c(!) f_c(r;!)$, where $c(!)$ is the DOS of the tip, and $f_c(r;!)$ = $(1/\pi) \text{Im} V_c(r;!)$. $G_{ff}(!) V_c(r;!)$ is the analogue of the f electron DOS, which contains renormalized tunneling matrix elements between the tip and the adatom [12]. In a more standard form, the DC is

$$G(r;!)=2e^2t_c^2\sim\frac{q\bar{q}}{2+1}+\frac{(q+q^S)}{2+1}; \quad (12)$$

where e is the electron charge, $! = +eV$, with eV the applied bias, $\bar{q}(r;!)=\frac{1}{2}(!)=\text{Im} f_{ff}(r;!)$, where $(!)$ is the graphene DOS per spin, and $(r;!)=\frac{1}{\pi}[\text{Re} f_{ff}(r;!)] = \text{Im} f_{ff}(r;!)$; $q(r;!)=\text{Re} V_c(r;!)=t_c(z)V(!)$ and $(r;!)=\text{Im} V_c(r;!)=t_c(z)V(!)$ are the Fano parameters [7]. In contrast with usual metal surfaces, the Fano factor q has a live dependence with the bias in graphene. The conjugate forms $q(r;!)$ and $(r;!)$ are defined by the conjugate tunneling matrix element $V_c(r;!)$. In the particular case when the tip is above the adatom ($R=0$), $q=q$ and $=q^S$ and $q^S=[V_c+(t_c(z)V)\text{Re} \frac{A^S}{f_{ff}}(!)]/[t_c(z)V(!)]$; where $\frac{A^S}{f_{ff}}(!)$ is defined by Eq.(6), and $A^S=1$. In the case where the adatom and the tip are on top of each other in the center of the hexagon, destructive interference leads to cancellation of the perturbative corrections on the tunneling matrix element in Eq.(11), and the Fano parameter simplifies to $q^S=V_c/[t_c(z)V]$ and $^S=0$. For adatoms with d and f -wave orbitals, the cancellation is not exact.

The shape of the Fano resonances in the DC curves is driven by the ratio q^S . When $q^S=1$, the DC

curve shows a pronounced peak, whereas in the opposite regime, $q^S=1$ one expects a dip. For a set of parameters $V=1\text{eV}$, $U=1\text{eV}$, $V_D=4\text{eV}$, $V_D=2\text{eV}$, $V_D=0.1\text{eV}$ and $V_D=0.5\text{eV}$, in the asymmetric case, for $V_c/t_c=0.1$, the red curve shown in the inset of Fig. 2(a) has a small dip, which is suppressed when $V_c/t_c=0.2$. In contrast, the curves shown in Fig. 2(b) for the symmetric case have a well pronounced peak for all finite values of q^S [see inset of Fig. 2(b)], reflecting the fact that $q^S=1$ is always large ($^S=0$). Fig. 2(a), (b) and 2(c), (d) compare the features of the positive bias resonance for $t_c=0.15\text{eV}$ and $t_c=0.02\text{eV}$, respectively. All red curves in Fig. 2 correspond to $V_c/t_c=0.1$. Increasing this ratio from $V_c/t_c=0.25$ up to 1.6 , the DC curves show two strongly pronounced peaks indicating the position of the two magnetic Fano resonances at V_D+nU and $V_D+n_\#U$. For $V_c/t_c<0.1$, in the asymmetric case, Fig. 2(c) shows an inversion in the structure of the resonance ($V_c/t_c=0.01$) for positive bias. The shape of the DC curves for small q^S [see insets of Fig. 2] agrees with a recent STM measurement of the Kondo peak in graphene [13].

The decrease in the separation of the peaks with increasing V_c reflects the suppression of the local moment by the proximity of the STM tip. In particular, in the symmetric case [Fig. 2(b)], the hybridization of the adatom with graphene is weaker than in the asymmetric one, making local moment much more sensitive to the STM tip. The difference is indicated clearly by the separation of the peaks for large V_c and also by the width of the peaks as V_c goes to zero. In the asymmetric case (Fig. 2(a)), the peaks remain broad at small V_c whereas in the other case their width collapses much faster, reflecting their anomalous broadening $\propto |j|^2=t^2$ [see Eq. (8)]. In the opposite limit, for V_c large enough, the two DC magnetic peaks eventually merge on top of each other, destroying the local moment completely. The merging of the peaks happens much earlier in the symmetric case [Fig. 2(b)] than in the asymmetric one. We note that for large V_c , fluctuations drive the DC away from equilibrium (although still in the perturbative regime for $V_c \ll V$), invalidating the strict applicability of Eq. (12). The

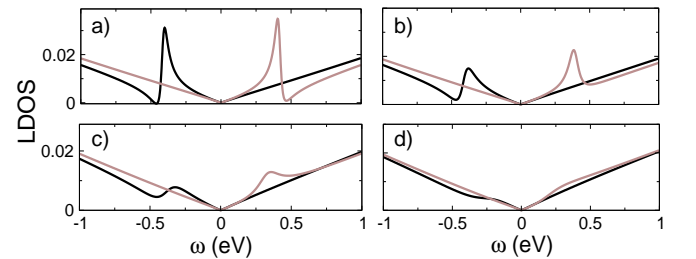


FIG. 3: Graphene LDOS at the adatom site (top carbon case) for $V_c/t_c = 0.1; 0.7, 1.1$ and 1.6 , from (a) to (d) ($t_c = 0.15\text{eV}$). Black curve: $n=$; brown: $n_\#$. Total LDOS: $n=+n_\#$.

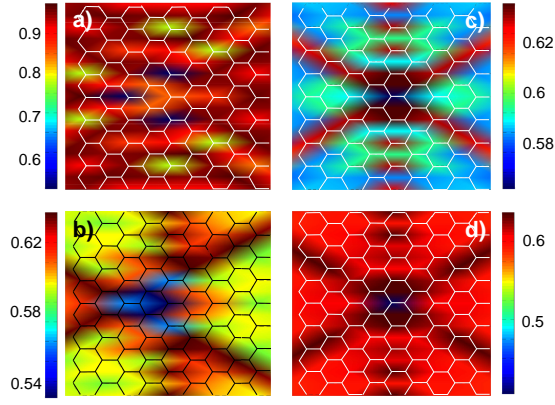


FIG. 4: Integrated LDOS maps around the adatom (center) in the asymmetric case, with the adatom on top of the carbon. On the left (right): scans for the opposite (same) sublattice of the adatom: (a), (c) without ($t_c = V_c = 0$) and (b), (d) with the tip ($t_c = 0.2 \text{ eV}$, $V_c = 0.02 \text{ eV}$).

main effect of fluctuations, however, is to further suppress the local moment, and in this sense the equilibrium calculation may be regarded as a conservative estimate for the main effect, the suppression of the local moment by the STM tip. As the tip separation to the adatom becomes progressively small the DC peaks can shift strongly: in that case, the peak on the right will red shift and eventually cross the experimentally accessible bias window around the Fermi level, providing an experimental signature for the presence of the local moment with a non-magnetic tip, regardless the presence of the Kondo peak. A significant suppression of the local moment by the metallic tip is harder for adatoms with a very large U , such as cobalt, which show a large local moment when hybridized with metals, but may be easily achieved in adatoms which are not usually magnetic and exhibit a local moment in graphene [4].

The Fano resonance also generates magnetic peaks in the LDOS around the adatom. The plots in Fig. 3 show the evolution of those peaks with the increase of V_c in the asymmetric case, for up and down spins. As the level is broadened by the tip, the height of the peaks clearly collapses [Fig. 3(d)].

In the case where the adatom is on top of the carbon, the sublattice asymmetry in the LDOS provides another STM signature that identifies the position of the adatom in the lattice. The LDOS for the asymmetric case can be computed perturbatively for small t_c and V_c ,

$$\begin{aligned} \rho_{x; \uparrow}^{\text{AS}}(r; \epsilon) &= 1 - (V^2) \text{Im} \left[\rho_{ff; \uparrow}^{\text{AS}}(z; \epsilon) \right]_{V_c=0} \quad (1 =) \\ &\quad \text{Im} \left[\rho_x(r; \epsilon) G_{ff; \uparrow}^R(\epsilon) \right] \rho_x(r; \epsilon); \quad (13) \end{aligned}$$

where $x = b$ for the same sublattice of the adatom and $x = a$ for the opposite one. The first term is the renor-

malized LDOS in the absence of the adatom and

$$\rho_x(r; \epsilon) = V G_{xb}^{\text{OR}}(R; \epsilon) + \frac{t_c(z) G_{aa}^{\text{OR}}(0; \epsilon)}{V_c^{\text{AS}}(r; \epsilon)} \rho_{ff}^{\text{AS}}(r; \epsilon)$$

contains the interference effects due to the interplay of the adatom and the tip in graphene. ρ_x in Eq. (13) follows by exchanging G_{xb}^0 by G_{bx}^0 and V_c^{AS} by V_c^{AS} [see Eq. (10)]. The STM topography maps computed from integration of Eq. (13) in energy (see Fig. 4) clearly show the asymmetry between the two sublattices (the adatom has three nearest neighbors and six next nearest neighbors). Fig. 4(a), (b) display the integrated LDOS for the opposite sublattice of the adatom, which has a lower point group symmetry, while Fig. 4(c), (d) display similar maps for the same sublattice of the adatom, with and without interference effects from the tip.

In conclusion, we have derived the fingerprints for Fano resonances of magnetic adatoms in graphene. We have shown the signatures in the DC curves that identify the position of the adatom and possibly the presence of local moments, away from the Kondo regime.

We acknowledge E. Fradkin, K. Sengupta, H. Manoharan and E. Andrei for discussions. BU acknowledges partial support from U.S. Department of Energy under the grant DE-FG 02-91ER 45439 at University of Illinois, and the Aspen Center of Physics, where this work started. SWT acknowledges support from UC-Lab FRP under award number 09LR 05118602. AHCN acknowledges the partial support of the U.S. Department of Energy under the grant DE-FG 02-08ER 46512. During the preparation of this paper we became aware of a related work [14].

-
- [1] K. S. Novoselov et al., Nature 438, 197 (2005); Y. Zhang et al., Nature 438, 201 (2005); A. H. Castro Neto et al., Rev. Mod. Phys. 81, 109 (2009).
 - [2] E. Stolyarova et al., PNAS 104, 9209 (2007); G. M. Rutter et al., Science 317, 219 (2007); V. Barar et al., Appl. Phys. Lett. 91, 122102 (2007); M. Ishigami et al., Nano Letters, 7, 1643 (2007); Y. Zhang et al., Nat. Phys. 4, 627 (2008); V. Geringer et al., Phys. Rev. Lett. 102, 076102 (2009); G. Li et al., Phys. Rev. Lett. 102, 176804 (2009).
 - [3] D. M. Eigler et al., Nature 344, 524 (1990).
 - [4] B. Uchoa et al., Phys. Rev. Lett. 101, 026805 (2008).
 - [5] K. Sengupta et al., Phys. Rev. B 77, 045417 (2008).
 - [6] D. W. Mitho and E. Fradkin, Phys. Rev. Lett. 64, 1835 (1990); G. M. Zhang et al., Phys. Rev. Lett. 86, 704 (2001); M. Hentschel et al., Phys. Rev. B 76, 115407 (2007); B. Dora et al., Phys. Rev. B 76, 115435 (2007).
 - [7] U. Fano, Phys. Rev. 124, 1866 (1961).
 - [8] A. V. K. rashennikov et al., Phys. Rev. Lett. 102, 126807 (2009).
 - [9] The hybridization in Eq. (3) can be easily generalized for d and f-wave representations of the localized orbital, and also for substitutional impurity defects.
 - [10] P. W. Anderson, Phys. Rev. 124, 41 (1961).

- [11] The non-linear corrections of the spectrum give a finite
but small renormalization of the level, ϵ_0 , for $j \neq j_0$.
- [12] M. P. M. Halet al. Phys. Rev. B 63, 085404 (2001).
- [13] H. M. Anoharan et al. (unpublished).
- [14] K. Saha et al., arXiv:0906.2788 (2009).